Steric Effects in S_N2 Reactions. The Influence of Microsolvation

Adel Ahmed Mohamed[†] and Frank Jensen*[,‡]

Department of Chemistry, Faculty of Science, Helwan University, Helwan, Cairo, Egypt, and Department of Chemistry, SDU Odense University, Campusvej 55, DK-5230 Odense M, Denmark

Received: August 2, 2000; In Final Form: December 12, 2000

Ab initio molecular orbital calculations at the B3LYP/6-31+G* and MP2/6-31+G* levels have been performed to study the effect of microsolvation on the S_N2 reaction profile for $Cl^- + RCl$ (R = methyl, ethyl, i-propyl, and *tert*-butyl). Microsolvation corresponding to 0−4 water molecules, and 0−2 molecules of methanol, acetonitrile, acetone, dimethyl ether and propane has been investigated. The polarizable continuum solvent model has been used to investigate the effect of bulk solvation. The calculated barrier heights increase with the number of solvent molecules and the size of the R group. Microsolvation causes only small changes in the TS geometries for the methyl, ethyl, and i-propyl systems, whereas the *tert*-butyl TS becomes significantly looser. Microsolvation decreases the steric effect, with the modulation depending on the dielectric constant of the solvent. For water, the decrease in steric effect is shown to be due to an increased solvation of the TS, mediated by the electron donating effect of the methyl group. The polarizable continuum solvent model in general underestimates changes in steric effects due to solvation.

I. Introduction

Bimolecular nucleophilic substitution (S_N2) reactions of the type

$$X^- + RY \rightarrow XR + Y^- \qquad (1)$$

have been the subject of much theoretical and experimental research due to their role in developing fundamental ideas in physical organic chemistry.[1−3] It has been established that in solution the relative rates of RY, with R being different alkyl groups, are relatively constants for a variety of Y.[4,5] The main influence of substituents on the reaction rate is due to bulky R-groups hindering the reaction by inhibiting the approach of the nucleophile to the central atom. This is commonly referred to as a steric effect, and in this paper we take the methyl system as the reference point. For gas-phase reactions, the same ordering with respect to R is found, although the steric effect appear to be larger by roughly a factor of two than that in solution.[6]

The surrounding medium influences most chemical processes. The gas and solution phase rates for S_N2 reactions involving halogen exchange typically differ by 20 orders of magnitude.[7] Bohme and Rasket[8] have found differences of nearly 3 orders of magnitude in reaction rates when the reaction takes place in the presence of up to three water molecules. Solute−solvent interactions not only affect the dynamics of chemical reactions but also modify the potential energy surface (PES). Various models have been used to investigate such interactions.[9] The effects of solvent on the PES are either direct effects, corresponding to energy shifts of critical points[10] or changes in the position of the critical points due to geometry relaxation.[11] Furthermore, solvent also causes changes in the shape of the PES around the critical points leading to new vibrational levels.[12]

In the gas phase, reaction 1 has a double-well potential with minima corresponding to ion−dipole complexes separated by a central energy barrier. Experimental studies have shown that shallow ion−dipole complexes are also observable in acetonitrile,[13] but addition of methanol causes the complexes to disappear.[14] In DMF an energy well is computed for the ion−dipole complex,[15] but it is almost nonexistent in water.[16] In all these cases, the minima are very shallow, and the most prominent feature is the central barrier. The solvent may also alter the structure of the transition state to be tighter or looser. For reactions with high barriers, solvation will cause transition structures to be looser than in the gas phase. Conversely, when the barrier is small, the transition structure will experience only a small change in geometry upon solvation, as for example in S_N2 reactions of CH_3X.[3]

Nucleophilic substitution reactions have been studied extensively in solution.[17] The solvent effects on the profile of reaction 1 have been studied theoretically by classical molecular dynamics,[18] Monte Carlo,[16] integral equation theory[19] and the polarizable continuum model.[20] Okuno[21] has applied microscopic reaction theory and found that the free energy of activation for the microsolvated reaction 1 with four water molecules gives good agreement with the activation energy for the corresponding reaction in bulk water. Constentin and Saveant have compared S_N2 and electron-transfer mechanisms for the reaction of NO^- with RCl with continuum solvent models.[22]

The aim of the present work is to investigate the influence of microsolvation on the steric effects of the $Cl^- + RCl$ S_N2 reaction, with R being methyl, ethyl, i-propyl, and *tert*-butyl. We have previously studied the steric effect in the corresponding gas-phase reactions at the MP2/6-31G* level of theory.[23] Our main focus in the present paper is on microsolvation by water, because it is one of the most extreme solvents, and furthermore small enough to allow addition of several solvent molecules. We have also included a smaller study of microsolvation by two molecules of methanol, acetonitrile, acetone, dimethyl ether, and propane.

For comparison purpose we have considered only the S_N2 reaction of *tert*-butyl chloride, although a substitution reaction

* Corresponding author: E-mail: frj@dou.dk.
[†] Helwan University.
[‡] SDU Odense University.

10.1021/jp002802m CCC: $20.00
Published on Web 02/15/2001

in reality is likely to occur by an S_N1 mechanism.[24] We focus on the energetics (enthalpy) of the reaction profile, because an adequate treatment of entropy (free energy) would require a sampling of many solvent configurations. Furthermore, we will concentrate on the lowest energy configuration for each microsolvated system.

In section II, the computational details are described followed by results for water as a solvent in section III, other solvents in section IV, and discussion in section V. The conclusions are given in the final section.

II. Computational Details

Ab initio molecular orbital calculations were carried out for the microsolvated cluster reactions

$$Cl^-\cdot(S)_n + RCl \rightarrow ClR + Cl^-\cdot(S)_n$$

using the Gaussian 98[25] series of programs. For S = water we have considered $n = 0-4$, while for S = methanol, acetonitrile, acetone, dimethyl ether, and propane only $n = 0-2$ was investigated. Geometry optimizations were performed at the DFT level using Becke's three-parameter hybrid method,[26] B3LYP. The 6-31+G*[27] basis set is used throughout this study. Harmonic frequencies have been calculated to confirm the nature of transition structures. Single-point energies with second-order Møller−Plesset perturbation theory (MP2) at B3LYP/6-31+G* geometries were calculated with the same basis set. The MP2 and B3LYP methods give similar results for complexation and relative activation energies, and only the B3LYP results are discussed in detail. Although enthalpy and entropy corrections due to finite temperature can be calculated within the rigid-rotor harmonic-frequency approximation, the presence of many low-lying frequencies in the clusters makes this approach less accurate, especially for the entropy. Relative activation energies based on electronic energies are therefore compared to experimental relative activation energies, avoiding the entropic problem. As shown in the Supporting Information, the enthalpy corrections (mainly zero point energies) are small and do not change the conclusions based on electronic energies.

Deng et al.[28] have provided a critical analysis of the performance of DFT methods in calculating equilibrium and transition state properties of gas-phase S_N2 reactions $X^- + CH_3X$ for X = F, Cl, Br, and I. They found that local VWN and nonlocal BP DFT methods underestimate the barrier height. On the other hand, both the B3LYP and BH&HLYP methods have been found to give quite accurate transition state information.[29]

For studying microsolvated cluster reactions that include large R groups and several solvent molecules, we have selected DFT due to its combination of accuracy and low CPU cost. Other work has shown that the B3LYP method works well for hydrogen bonds and that B3LYP/6-311++G** or B3LYP/6-311+G* led to results similar to those obtained by the MP2/6-311++G** method.[30] For the water dimer, the B3LYP method gives geometries, energies, and frequencies in close agreement with MP2 and experimental results.[31] B3LYP calculations with large basis sets give a dimer binding energy of −4.6 kcal/mol, 0.5 kcal/mol smaller than the MP2 value with same basis set and 0.8 kcal/mol smaller than the experimental value.[31−34] The calculated B3LYP/6-31+G* O−O bond length in the water dimer is 2.75 Å, slightly less than the experimental value of 2.98 Å,[35] with a calculated binding energy of −4.6 kcal/mol.[31]

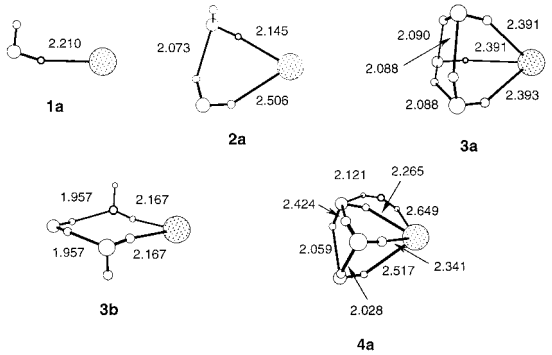

Figure 1. B3LYP/6-31+G* optimized geometries of $Cl^-\cdot(H_2O)_n$ complexes (distances in Å).

To account for the effect of long-range electrostatic interaction with the bulk solvent, the reactions were also studied with the polarizable continuum model (PCM),[36] using the default parameters.[25] In this model the solvent is represented as an infinite polarizable continuum surrounding a molecular shaped cavity. The molecular free energy of solvation ΔG_{sol} was calculated at geometries optimized in vacuo or microsolvated, using the B3LYP/6-31+G* level. The free energy of solvation ΔG_{sol} can be partitioned into electrostatic and nonelectrostatic components.

$$\Delta G_{sol} = \Delta G_{ele} + \Delta G_{dis} + \Delta G_{rep} + \Delta G_{cav}$$

The ΔG_{ele} represents the electrostatic interaction between the solute and continuum solvent. The other three terms correspond to the nonelectrostatic part where ΔG_{dis} is the dispersion energy, ΔG_{rep} represents solute−solvent repulsion, and ΔG_{cav} is the cavity formation energy.

Atomic charges have been calculated by the natural population analysis (NPA) method at the B3LYP/6-31+G* level.[37]

III. Results for Water as a Solvent

A. Chloride Ion−Water Clusters $Cl^-\cdot(H_2O)_n$. The B3LYP/6-31+G* geometries of the $Cl^-\cdot(H_2O)_n$ ($n = 1-4$) clusters are shown in Figure 1. The $n = 1$ cluster has C_s symmetry with Cl^- bonded to water through one of its hydrogens. A C_{2v} structure in which the Cl^- is bonded to both hydrogens is a transition state and higher in energy by 1.2 kcal/mol. Two similar types of structures were found for $F^-\cdot(H_2O)$[38] at the HF and MP2 levels using different basis sets. For the $n = 2$ cluster, the optimal structure has the two water molecules bonded to Cl^- via their hydrogens and an intermolecular hydrogen bond.

Three different structures were found for the $n = 3$ cluster, the most stable one, **3a**, is pyramidal in shape with the Cl^- ion at the top of the pyramid and the three water molecules at its base. Each of the three water molecules forms a hydrogen bond with Cl^- and one with an oxygen atom of another water molecule. The other two forms (only one, **3b**, is shown in Figure 1) are planar ring structures and are 1.1 kcal/mol higher in energy than **3a**. The greater stability of **3a** is attributed to more hydrogen bonding. Only one structure was obtained for the $n = 4$ cluster, **4a**, in which all four water molecules are coordinated to Cl^-. These results are in good qualitative agreement with previous works for $F^-\cdot(H_2O)_n$[38] and $Cl^-\cdot(H_2O)_n$,[21] $n = 1-4$, at the MP2 and HF levels.

The microsolvation energy, which is defined as the energy of the $Cl^-\cdot$water cluster relative to the energy of infinitely separated Cl^- and H_2O, is given in Table 1. The calculated value for the interaction with one water molecule is −14.9 kcal/mol

TABLE 1: Energies of Ion−Dipole Complexes (ΔE) and TSs ($\Delta E^{\ddagger}$) at the B3LYP and MP2 Levels of Theory with the 6-31+G* Basis Set (kcal/mol) Microsolvated with 0−4 Water Molecules[a]

	Cl^-	methyl		ethyl		i-propyl		*tert*-butyl	
n	ΔE	ΔE	$\Delta E^{\ddagger}$	ΔE	$\Delta E^{\ddagger}$	ΔE	$\Delta E^{\ddagger}$	ΔE	$\Delta E^{\ddagger}$
0		−9.5	−0.9	−10.0	2.7	−11.2	5.3	−12.3	11.7
		(−9.4)	(7.9)	(−10.8)	(11.6)	(−12.3)	(14.6)	(−13.7)	(23.0)
	[−71.6]	[−59.4]	[−50.0]	[−59.0]	[−50.1]	[−57.1]	[−50.5]	[−55.1]	[−50.6]
1	−14.9	−23.3	−10.3	−23.7	−7.2	−24.7	−4.8	−25.6	0.8
	(−15.4)	(−24.1)	(−2.8)	(−25.1)	(0.5)	(−26.3)	(3.4)	(−27.4)	(10.3)
	[−64.2]	[−53.4]	[−48.6]	[−53.0]	[−48.6]	[−51.4]	[−49.1]	[−49.8]	[−49.0]
2a	−30.0	−37.4	−19.9	−37.9	−16.8	−38.6	−14.9	−39.4	−10.0
	(−31.6)	(−39.7)	(−13.4)	(−40.7)	(−10.3)	(−41.5)	(−8.0)	(−42.4)	(−3.0)
	[−57.1]	[−47.6]	[−46.7]	[−46.7]	[−46.7]	[−45.8]	[−46.8]	[−44.2]	[−47.2]
2b			−22.2		−19.7		−17.6		
			(−16.8)		(−13.7)		(−12.4)		
			[−46.2]		[−46.5]		[−45.7]		
2c			−18.9						
			(−12.3)						
			[−49.4]						
3a	−46.0	−52.8	−30.6	−53.1	−27.8	−53.8	−26.0	−54.4	−22.0
	(−48.9)	(−56.1)	(−25.2)	(−56.9)	(−22.2)	(−57.8)	(−20.2)	(−58.8)	(−16.6)
	[−48.1]	[−39.3]	[−44.8]	[−38.9]	[−44.2]	[−37.8]	[−44.0]	[−36.6]	[−45.1]
3b	−44.9	−51.0	−35.0		−33.8				
	(−47.5)	(−54.9)	(−31.1)		(−29.6)				
	[−54.4]		[−41.3]		[−38.9]				
3c			−33.2						
			(−28.5)						
			[−45.2]						
4a	−57.8	−66.2		−64.3		−64.7	−34.4	−65.3	−33.9
	(−62.2)	(−71.0)		(−69.8)		(−70.5)	(−29.9)	(−71.4)	(−30.6)
	[−48.4]	[−38.8]		[−40.2]		[−39.3]	[−43.1]	[−37.9]	[−41.2]
4b			−51.6		−49.1				
			(−49.8)		(−46.9)				
			[−35.1]		[−35.8]				
4c			−41.1						
			(−37.5)						
			[−39.8]						

[a] Values in parentheses correspond to MP2/6-31+G*//B3LYP/6-31+G* results. Values in brackets correspond to B3LYP/6-31+G* PCM free energies of solvation.

at the B3LYP level and −15.4 kcal/mol at the MP2 level, compared to the experimental value of −13.1 kcal/mol.[39] For the $Cl^-\cdot(H_2O)_2$ complex, the microsolvation energy is −30.0 and −31.6 kcal/mol at the B3LYP and MP2 levels, respectively. The stabilizations by addition of the second water molecule are thus −15.1 and −16.2 kcal/mol, respectively, which are somewhat higher than obtained by others[40] using the MP2/6-31G** level, but compare well with experimental results in the −12.6 to −13.0 kcal/mol range.[39] The microsolvation energy for $Cl^-\cdot(H_2O)_3$ calculated at the B3LYP level is −46.0 kcal/mol, giving a value of −16.0 kcal/mol for addition of a third water molecule. The increase in energy on successive addition of water molecules is attributed to the increased number of hydrogen bonds between water molecules in the cluster. The change in microsolvation energy resulting from addition of the fourth water molecule is less, −11.8 kcal/mol, due to the fact that the fourth water molecule is more loosely coordinated to the Cl^- ion, Figure 1.

The solvation free energies of the Cl^- ion and its corresponding water clusters were calculated with the PCM model as mentioned in section II. The solvation free energy of the Cl^- ion is calculated to be −71.6 kcal/mol (Table 1), which is slightly less than the experimental value of −75.0 kcal/mol.[41] At least part of this underestimation may be due to the valence electrons in the Cl^- ion being quite diffuse, resulting in a noticeable electron distribution outside the cavity.[42] The free energies of solvation of the $Cl^-\cdot(H_2O)_n$ clusters decrease with increasing number of water molecules, as expected. The total ΔG_{sol} can be decomposed into electrostatic and nonelectrostatic part (Table 2). The nonelectrostatic part is minor compared to the electrostatic part, but increases with the number of water molecules, whereas the electrostatic part decreases.

B. The Cl^- + RCl Gas-Phase Reactions. The geometrical parameters of the $Cl^-\cdot CH_3Cl$ complex are given in Figure 2. The complex has C_{3v} symmetry, and the nonbonded C−Cl bond length, 3.05 Å, is shorter than calculated at the MP2/6-31G*[23,42] and HF levels,[21] 3.16 and 3.27 Å, whereas the bonded C−Cl (1.86 Å) is longer compared with the other two levels, 1.81 and 1.83 Å, respectively. Similar results have been obtained using the 6-31+G** basis set.[42] Geometries of the $Cl^-\cdot$RCl complexes for the ethyl, i-propyl, and *tert*-butyl systems are provided as Supporting Information and show increase in both C−Cl distances upon methyl substitution (distances of 1.86, 1.89, 1.93 Å and 3.45, 3.86, 3.93 Å, respectively).

The calculated B3LYP/6-31+G* complexation energies for the methyl, ethyl, i-propyl, and *tert*-butyl systems are −9.5, −10.0, −11.2, and −12.3 kcal/mol, respectively, and −9.4, −10.8, −12.3, and −13.7 kcal/mol at the MP2 level, Table 3. These values are in good agreement with those calculated at the MP2/6-311+G**//MP2/6-31G* level,[23] and with experimental values of −8.6[43] or −12.2[44] kcal/mol for the methyl system, and −14.3 kcal/mol[43] for the *tert*-butyl system.

TABLE 2: Components of Solvation Free Energies (kcal/mol) for the Reactant, Transition States, and Ion Complexes for the $Cl^- + RCl$ Reaction in Water Obtained by the PCM Method at the B3LYP/6-31+G* Level of Theory

		ion complex		TS	
R	n	electrostatic	nonelectrostatic	electrostatic	nonelectrostatic
Cl^-	0	−71.6	0.1		
	1	−65.8	1.6		
	2	−60.4	3.3		
	3	−59.4	4.9		
	4	−55.2	6.8		
Me	0	−61.7	2.3	−52.1	2.1
	1	−57.5	4.1	−52.5	3.9
	2	−53.5	5.9	−52.3	5.4
	3	−47.0	7.7	−52.1	7.3
	4	−48.2	9.4	−45.0[a]	9.9[a]
Et	0	−61.5	2.5	−52.4	2.3
	1	−57.4	4.4	−52.8	4.2
	2	−53.2	6.5	−52.9	6.1
	3	−46.8	7.9	−52.1	7.9
	4	−50.2	10.0	−46.0[a]	10.2[a]
i-Pr	0	−60.4	3.3	−53.5	3.0
	1	−56.5	5.1	−53.9	4.8
	2	−52.7	6.9	−53.9	7.1
	3	−46.4	8.6	−52.9	8.9
	4	−49.8	10.5	−54.1	11.0
t-Bu	0	−58.9	3.8	−54.4	3.8
	1	−55.3	5.5	−55.1	6.1
	2	−51.7	7.5	−55.7	8.5
	3	−45.6	9.0	−55.6	10.5
	4	−49.1	11.2	−53.9	12.7

[a] **b** type structure.

The TS for the reaction of Cl^- with CH_3Cl has D_{3h} symmetry with C−Cl bond lengths of 2.37 Å, Figure 3. This is slightly longer than obtained at the MP2/6-31G*[23] level, 2.30 Å, but very similar to that obtained at the B3LYP/6-31+G** level.[42] The corresponding ethyl, i-propyl, and *tert*-butyl TSs are shown in Figures 4−6. The ethyl and *tert*-butyl TSs have C_s symmetry, whereas that of i-propyl has C_{2v} symmetry, in agreement with MP2/6-31G* calculations.[23] The two C−Cl bonds at the TS for the ethyl and *tert*-butyl systems are unequal, but the difference is small, 0.06 and 0.04 Å, respectively. In the gas phase the TS C−Cl bond lengths increase by 0.07, 0.17, and 0.47 Å relative to methyl along the ethyl, i-propyl, *tert*-butyl series, i.e., the TS become significantly looser by methyl substitution.

The experimental activation energy of the $Cl^- + CH_3Cl$ reaction is difficult to measure accurately, but it is known to be close to zero.[45] A value of 1 ± 1 kcal/mol was obtained by fitting experimental data to the RRMK model.[46] Calculations at CCSD[47] and MP2[23] levels of theory gave values of 3−10 kcal/mol, while the MP4/6-311+G** value is 1.3 kcal/mol.[23] Truong and Stefanovich[42] found an activation energy of −1.3 kcal/mol at the B3LYP/6-31+G** level. Our activation energies calculated at the B3LYP and MP2 levels are −0.9 and 7.9 kcal/mol, respectively. The B3LYP slightly underestimates the activation energy, but MP2 significantly overestimates the value.

The activation energies for the series are −0.9, 2.7, 5.3, and 11.7 kcal/mol at the B3LYP level and 7.9, 11.6, 14.6, and 23.0 kcal/mol at the MP2 level, respectively. The MP2/6-311+G**//MP2/6-31G* results for the same series are 2.3, 5.7, 8.6, and 18.2 kcal/mol, respectively.[23] Although the absolute values depend on the theoretical method, the relative activation energies are insensitive to the level of theory, Table 4. As there are no experimental results for the $Cl^- + RCl$ system, except for R = methyl, we compare our theoretical results with the experimental data for the closely related gas-phase $Cl^- + RBr$ reaction.[6,48] This reaction is close to thermoneutrality, and the TS should thus be fairly symmetric with respect to bond-breaking/formation. The results of the experimental gas-phase $Cl^- + RBr$ reactions[6] compare well with our results.

TABLE 3: Complexation (ΔE) and Activation Energies ($\Delta E^{\ddagger}$) at the B3LYP and MP2 Levels of Theory with the 6-31+G* Basis Set (kcal/mol) Microsolvated by 0−4 Water Molecules[a]

	Me		Et		i-Pr		t-Bu	
n	ΔE	$\Delta E^{\#}$	ΔE	$\Delta E^{\#}$	ΔE	$\Delta E^{\#}$	ΔE	$\Delta E^{\#}$
0	−9.5	−0.9	−10.0	2.7	−11.2	5.3	−12.3	11.7
	(−9.4)	(7.9)	(−10.8)	(11.6)	(−12.3)	(14.6)	(−13.7)	(23.0)
	[3.1]	[21.2]	[3.8]	[25.4]	[4.7]	[27.7]	[5.2]	[33.8]
1	−8.4	4.5	−8.8	7.7	−9.8	10.1	−10.7	15.7
	(−8.7)	(12.6)	(−9.6)	(14.9)	(−10.9)	(12.0)	(−12.0)	(25.7)
	[2.8]	[20.6]	[3.5]	[24.5]	[4.3]	[26.5]	[4.8]	[32.0]
2a	−7.4	10.1	−7.9	13.2	−8.6	15.1	−9.4	20.0
	(−8.1)	(18.2)	(−9.1)	(21.3)	(−9.9)	(23.6)	(−10.8)	(28.6)
	[2.5]	[20.8]	[3.8]	[24.7]	[4.0]	[26.8]	[4.5]	[31.0]
2b		7.8		10.3		12.4		
		(14.8)		(17.9)		(19.2)		
		[19.2]		[22.1]		[25.1]		
2c		11.8						
		(19.3)						
		[19.9]						
3a	−6.8	15.4	−8.1	18.2	−7.8	20.1	−8.4	24.1
	(−7.3)	(23.7)	(−8.1)	(26.6)	(−8.9)	(28.7)	(−9.9)	(32.3)
	[2.5]	[19.2]	[3.3]	[23.3]	[3.9]	[25.5]	[4.2]	[28.2]
3b	−4.9	11.1		12.3				
	(−6.1)	(17.7)		(19.2)				
		[18.3]		[22.7]				
3c		12.9						
		(20.4)						
		[16.3]						
4a	−8.5		−6.5		−6.9	23.3	−7.5	23.9
	(−8.8)		(−7.8]		(−8.3)	(32.3)	(−9.2)	(31.5)
	[1.6]		[2.9]		[3.5]	[30.0]	[4.1]	[32.2]
4b		6.2		8.7				
		(12.4)		(15.3)				
		[19.9]		[22.5]				
4c		14.6						
		(24.7)						
		[23.7]						

[a] Values in parentheses correspond to MP2/6-31+G*//B3LYP/6-31+G* results. Values in brackets correspond to B3LYP/6-31+G* PCM results.

C. The Microsolvated Reactions $Cl^-\cdot(H_2O)_n + CH_3Cl$. Figure 2 shows the structures of the complexes $(H_2O)_nCl^-\cdot CH_3Cl$, ($n = 1-4$). The water molecules coordinate to the more negatively charged chlorine atom with geometries similar to the corresponding $Cl^-\cdot(H_2O)_n$ complexes. Similar structures have been obtained at the HF/6-31G* level.[21] Microsolvation decreases the bonded C−Cl lengths and increases the nonbonded C−Cl lengths. The difference in bond distances between the gas and microsolvated phases increase with the number of water molecules, which may be rationalized in terms of greater charge separation in solution.

The energy of the $n = 1$ complex relative to the gas-phase reactants is −23.3 kcal/mol, Table 1. The microsolvation energy of the complex is thus −13.8 kcal/mol, which is slightly less than for the Cl^- ion, −14.9 kcal/mol. The microsolvation energies of the $n = 2$, 3, 4 complexes give stabilizations of −14.1, −15.4, and −13.4 for each successive addition of water, which follows the trend for the Cl^- ion, except for $n = 4$. The latter is due to the fact that the fourth water molecule coordinates directly to Cl for the chloride ion itself, but forms part of a second solvation shell for the complex.

The optimized TS geometry for the $n = 1$ system, **T1**, is shown in Figure 3 and has the water coordinated to one of the chlorine atoms similar to the corresponding ion complex. A similar structure was found by Okuno,[21] Chandrasekhar et al.,[15]

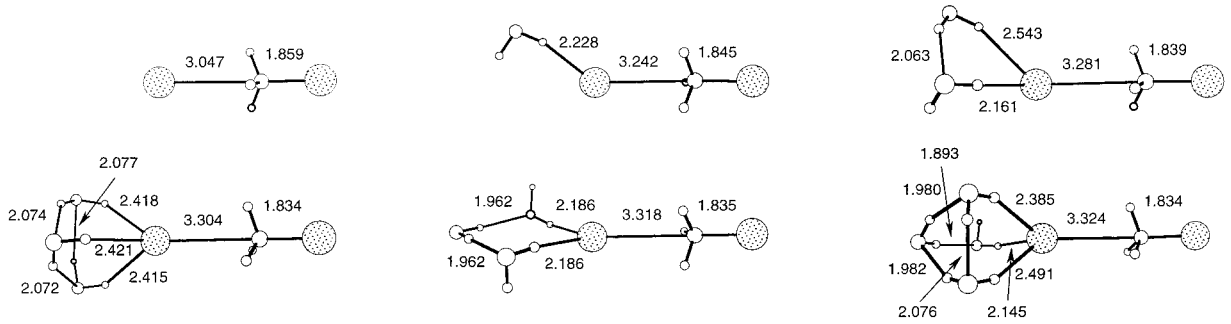

Figure 2. B3LYP/6-31+G* optimized geometries of $(H_2O)_nCl^-\cdot CH_3Cl$ complexes (distances in Å).

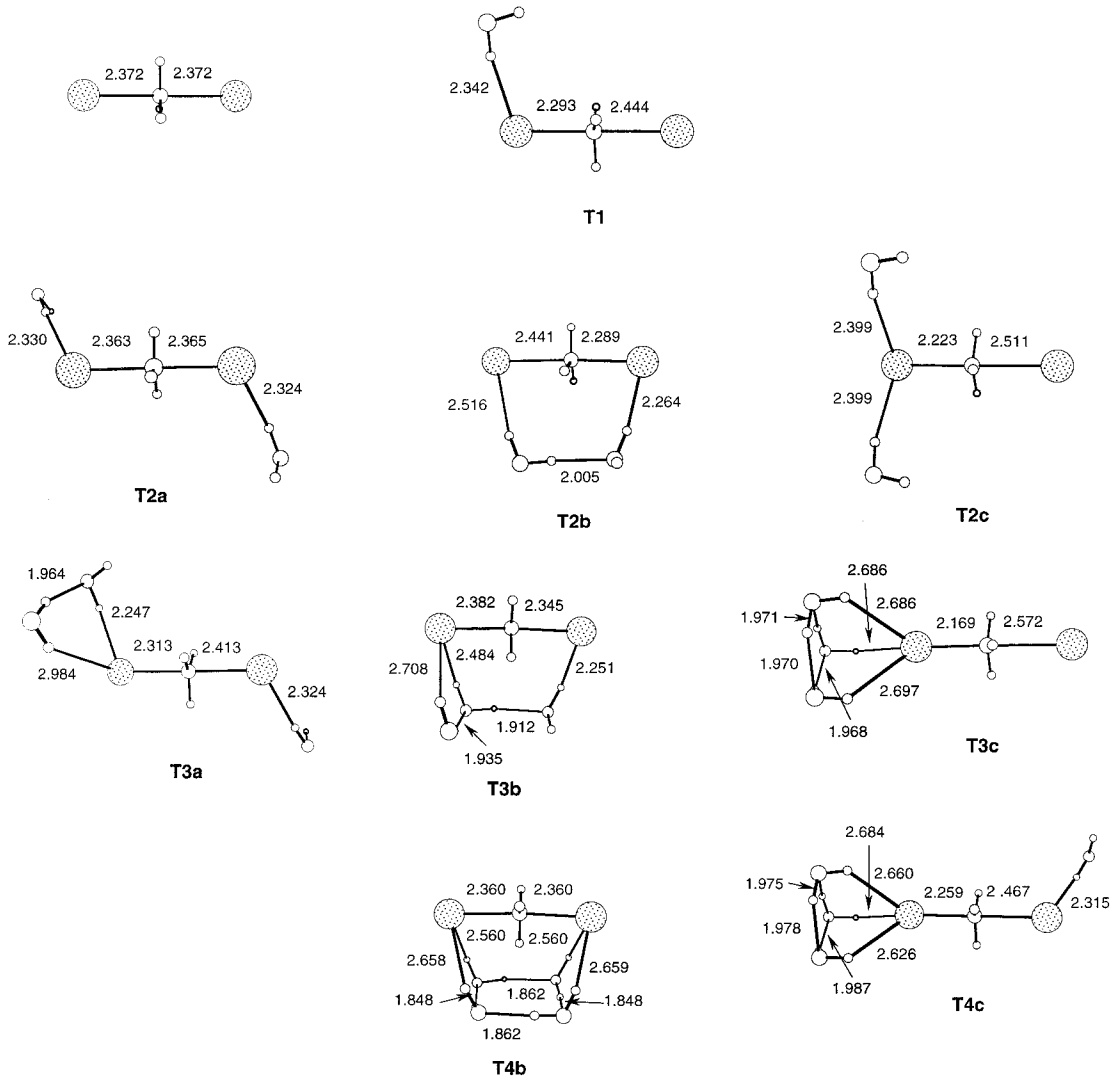

Figure 3. B3LYP/6-31+G* optimized geometries of microsolvated TSs for the S_N2 reaction of Cl^- with CH_3Cl (distances in Å).

Morokuma,[49] and Tucker and Truhlar.[40] A symmetric structure found by Tucker and Truhlar[40] corresponding to the water molecule bridging the two Cl^- ions was not found at the B3LYP level. Solvating the TS shortens one of the C−Cl bond distances from 2.37 to 2.29 Å and elongates the other to 2.44 Å, Figure 3. This is at least partly a consequence of breaking the reaction symmetry, i.e., the monohydrated reaction is no longer thermoneutral. The distance between the Cl^- and water molecule increases from 2.23 Å in the ion complex to 2.34 Å at the TS due to charge delocalization.

For the TS with $n = 2$, three different structures were optimized, Figure 3. The first, **T2a**, has one water molecule coordinated to each chlorine atom with nearly equal C−Cl bond lengths of 2.36 and 2.37 Å. Structure **T2b** has the two water molecules bridging the two chlorine atoms by hydrogen bonding. The third structure, **T2c**, has both water molecules coordinated to the same chlorine, resulting in asymmetric C−Cl bond lengths of 2.23 and 2.51 Å. The relative energies of the three TSs are 2.3, 0.0, 4.0 kcal/mol, Table 3. For the TSs with $n = 3$ and 4, there are similar balanced (**a** and **b**) and unbalanced types of structures (**c**), Figure 3. An **a** type structure, for the case of $n = 4$ obtained by Okuno[21] at the HF level, was not found at the B3LYP level, it collapses to **T4b** which maximizes the number of internal hydrogen bonds. For comparing with the situation in bulk solution, we consider the **a** type structures to be the best models, and we consequently focus on these results.

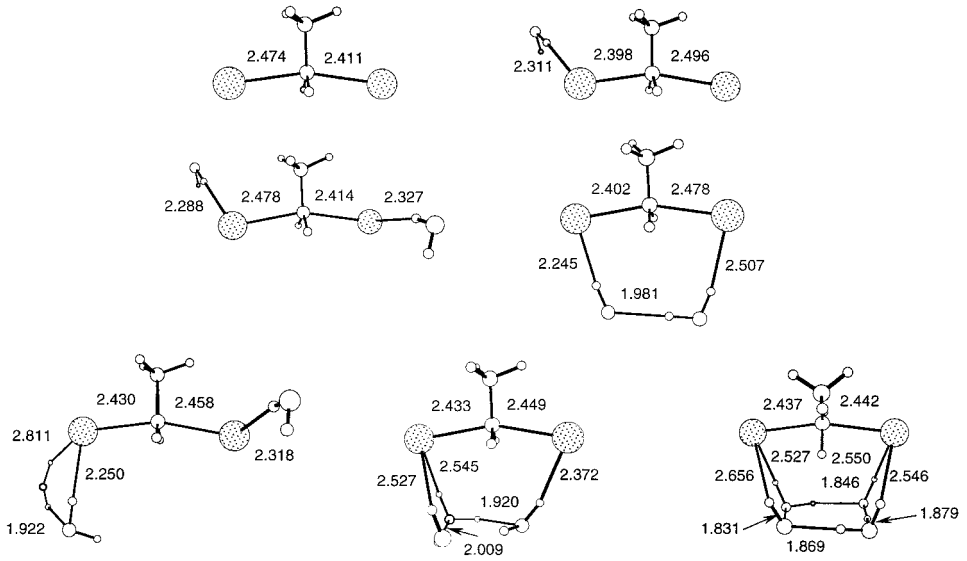

Figure 4. B3LYP/6-31+G* optimized geometries of microsolvated TSs for the S_N2 reaction of Cl^- with CH_3CH_2Cl (distances in Å).

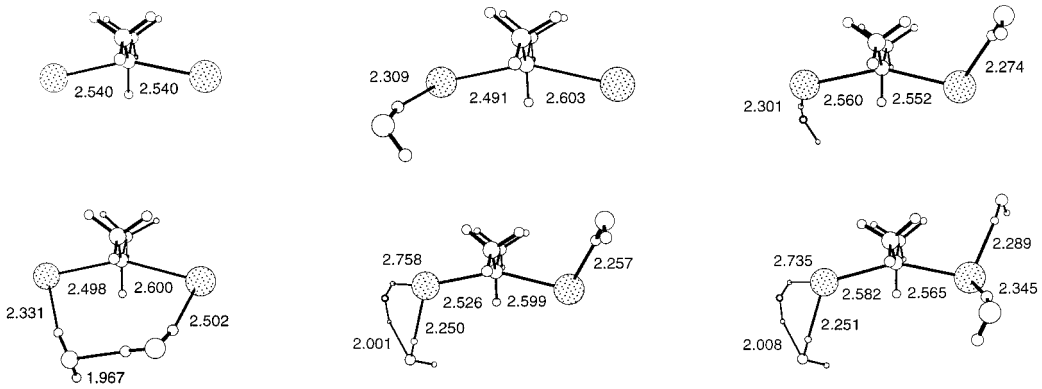

Figure 5. B3LYP/6-31+G* optimized geometries of microsolvated TSs for the S_N2 reaction of Cl^- with $(CH_3)_2CHCl$ (distances in Å).

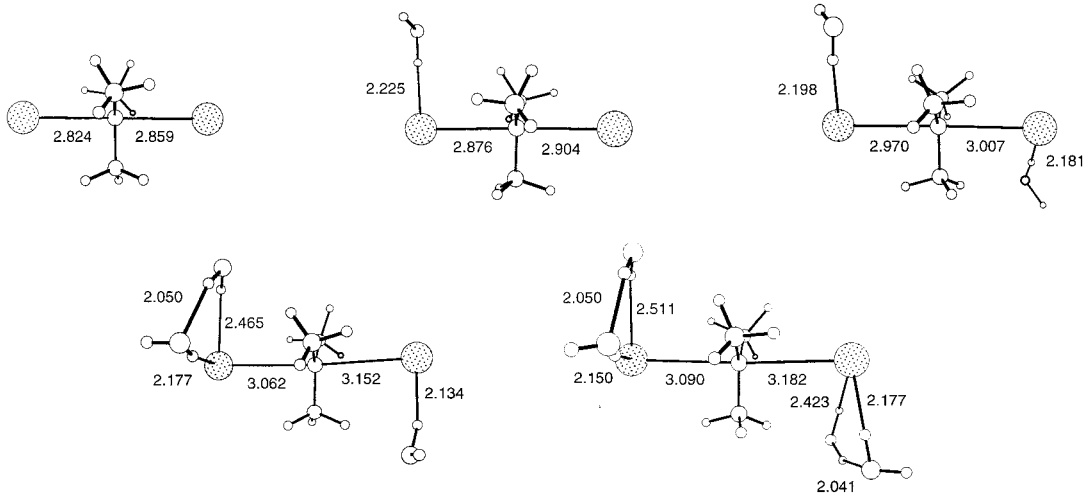

Figure 6. B3LYP/6-31+G* optimized geometries of microsolvated TSs for the S_N2 reaction of Cl^- with $(CH_3)_3CCl$ (distances in Å).

The microsolvation energy of the $n = 1$ TS, −9.4 kcal/mol (Table 1), is lower than the ion complex value of −13.8 kcal/mol, due to the charge delocalization. For the $n = 2$ TS, **T2a**, the microsolvation energy is −9.6 kcal/mol relative to the $n = 1$ TS, and is again lower than the ion complex value, −14.1 kcal/mol. The less effective solvation of the TS relative to the reactant and ion−dipole complex increases the activation energy relative to the reactants from the gas-phase value of −0.9 to 4.5, 10.1, and 15.4 kcal/mol (Table 3) for the **T1**, **T2a**, and **T3a** structures, respectively. The **T4b** structure is artificially low in energy due to the increased hydrogen bonding and is not directly comparable to the **a** type TSs. The activation energies can be compared to the experimental bulk value of 26.5 kcal/mol.[50] Single-point MP2 calculations give barrier height values of 7.9, 12.6, 18.2, and 23.7 kcal/mol for 0−3 water molecules, respectively. These values are significantly higher than the corresponding B3LYP level values but show the same trend. It is clear that in order to converge to the experimental

value many more water molecules are required. Calculations using a simple model for the water potential have shown that about 50 water molecules are required to converge the calculated barrier height.[51] A complete second solvation shell is probably necessary for providing a balanced description of the **a** and **b** type TSs.

The results of the PCM calculations are shown in Table 1. The free energy of solvation of CH_3Cl is −0.4 kcal/mol, which is in good agreement with the experimental value, −0.6 kcal/mol.[52] The PCM estimate of the free energy of solvation of the ion complex $Cl^-\cdot CH_3Cl$ is −59.4 kcal/mol while that of the TS is −50.0 kcal/mol, with the difference again due to differences in charge delocalization. With the PCM estimate, the complex is above the separated reagents, i.e., the reaction has a unimodal reaction profile with a calculated barrier of 21.2 kcal/mol. The activation energy (Table 3) is relatively independent of explicit microsolvation, with values of 20.6, 20.8, and 19.2 kcal/mol for $n = 1-3$, respectively. Table 2 shows that the electrostatic component is responsible for the difference between the complex and TS, but the nonelectrostatic component is significant as the number of explicit water molecules increases.

D. Microsolvated Reactions $(H_2O)_n\cdot Cl^- + RCl$, R = Ethyl, i-Propyl, *tert*-Butyl. The optimized geometries of the microsolvated ion-complexes of the ethyl, i-propyl, and *tert*-butyl systems are very similar to those for the methyl system and are provided as Supporting Information. The microsolvation energies (Table 1) of the ion complexes for the different systems with the same number of coordinated water molecules increase slightly, ∼2 kcal/mol, with the size of the R group. The calculated complexation energies are given in Table 3.

For the ethyl, i-propyl, and *tert*-butyl systems, only TSs of type **a** and **b** have been considered. Unbalanced structures in which all water molecules coordinate to only one chlorine have in other work been found to contribute very little to the overall reaction.[21] Figures 4−6 show the calculated geometries for the microsolvated TSs of the $Cl^- + RCl$ systems with R = ethyl, i-propyl, and *tert*-butyl. Solvent bridging structures corresponding to **T2b**, **T3b**, and **T4b** for the methyl case (Figure 3) were also found for the ethyl system with $n = 2, 3, 4$ and the i-propyl system with $n = 2$, but not for the *tert*-butyl case. For $n = 4$, the ethyl case only has a bridging structure **T4b**, whereas the i-propyl and *tert*-butyl systems give only **a** type structures.

For the ethyl TSs, the presence of water molecules does not appreciably change the gas-phase geometry, as is most evident by comparing the **T2a** structure with the gas-phase TS. The i-propyl TSs show a very slight elongation of the C−Cl distances by 0.01−0.02 Å upon addition of two water molecules, and an additional 0.02 Å increase by further addition of two water molecules. The *tert*-butyl system, in contrast, displays a significant loosening of the TS upon microsolvation, by 0.15 Å for two water molecules, and by additional 0.12−0.15 Å for four water molecules. It should also be noted that the hydrogen−chlorine distances decrease along the R = methyl, ethyl, i-propyl, *tert*-butyl series, indicating a strengthening of the interaction between the chlorines and water. The calculated microsolvation energies of the ethyl, i-propyl, and *tert*-butyl systems are given in Table 1. Methyl substitution increases the solvation energies slightly, but the trends are very similar to those for the methyl system and will not be discussed in detail.

IV. Other Solvents

To investigate the effect of changing the solvent, we have also performed calculations with methanol, acetonitrile, acetone, dimethyl ether, and propane as solvents. Because these are substantially larger than water, we have considered only one and two solvent molecules, and the latter only in a configuration corresponding to a balanced solvation of the TS. The calculated activation energies are shown in Table 5. For the less polar solvents the calculated effects are quite small, and we have thus also considered the effect of basis set superposition error. This has been estimated by the counterpoise (CP) method,[53] and the results are given in parentheses in Table 5. Most of the values are a few tenths of a kcal/mol and have little influence on the conclusions.

Similar to the case with water, the inclusion of solvent molecules increases the activation energy over the gas phase. The increase in activation energy correlates approximately with the macroscopic dielectric constant, i.e., water > methanol > acetonitrile > acetone > dimethyl ether > propane. The correlation is significantly nonlinear, with an initial steep increase in the activation energy, which levels off for high values of the dielectric constant. There also appears to be a smaller solvent-specific component related to hydrogen bonding, as the activation energies for methanol are slightly higher than for acetonitrile, despite the slightly larger dielectric constant for the latter.

Activation energies relative to the methyl system are shown in Table 6; for these relative results the CP corrections are substantially smaller. The effect of microsolvation again correlates approximately with the dielectric constant. The results for propane as a solvent are only marginally lower than in the gas phase. Dimethyl ether and acetone reduce the steric effect slightly, but the effect levels off as the dielectric constant increases. Analogous to the absolute value of the activation energy, there appears to be a solvent-specific component, i.e., methanol and water give a further reduction in the steric effect due to hydrogen bonding. This is analyzed further in the next section.

Geometries for the TSs follow that trend discussed for water as a microsolvent in the previous sections. The C−Cl distances change very little upon microsolvation for the methyl, ethyl, and i-propyl systems. For i-propyl, for example, the two C−Cl distances change from 2.540/2.540 Å to 2.536/2.551 Å by addition of two molecules of acetonitrile. The *tert*-butyl system, in contrast, displays a small elongation by microsolvation, i.e., from 2.82/2.86 Å to 2.88/2.88 Å by addition of two molecules of acetonitrile. The changes are thus analogous to microsolvation by water, but the effects are smaller and again correlate approximately with the solvent dielectric constant.

The PCM calculations for the absolute activation energy follow the trend from the microsolvation, i.e., a rapid increase as a function of dielectric constant, followed by a leveling off for larger values. Analogous to using water as a solvent, there is little difference between using the PCM method on the "naked" gas phase reaction or on the reaction where a few explicit solvent molecules are included. Relative activation energies, on the other hand, display little or no correlation with the dielectric constant, indicating that the PCM method may be problematic for calculating differences in solvation for sterically different reactions.

V. Discussion

The $Br^- + RBr$ and $Cl^- + RBr$ reactions have been studied experimentally in DMF[54] and acetone,[55,56] the corresponding relative activation enthalpies are given in Table 4. It should be stressed that the major reaction of *tert*-butyl halides is elimination, and only a small percentage of the total reaction is due to

TABLE 4: Relative Activation Energies for $X^- + RY$ Reactions (kcal/mol)[a]

R	$\Delta\Delta E^{\ddagger}$[b] X = Y = Cl $n = 0$	$n = 1$	$n = 2$	$n = 3$	$\Delta\Delta E^{\ddagger}_{gas}$[c] X=Cl Y=Br	$\Delta\Delta E^{\ddagger}_{DMF}$[d] X=Cl Y=Br	$\Delta\Delta E^{\ddagger}_{ace}$[e] X=Cl Y=Br	$\Delta\Delta E^{\ddagger}_{ace}$[f] X=Br Y=Br
Me	0.0	0.0	0.0	0.0	0.0	0.0	0.0	0.0
Et	3.6	3.2	3.1	2.8	3.3	1.3	1.9	1.7
	(3.6)	(3.3)	(3.1)	(2.9)				
	[4.3]	[3.9]	[3.9]	[4.1]				
i-Pr	6.1	5.5	5.0	4.6	7.6	3.1	3.1	3.9
	(6.7)	(6.2)	(5.4)	(5.0)				
	[6.6]	[6.0]	[5.9]	[6.3]				
t-Bu	12.6	11.2	9.9	8.6		3.3	5.3 (7.6)	6.0
	(15.1)	(13.1)	(10.3)	(8.6)				
	[12.6]	[11.4]	[10.2]	[9.0]				

[a] Theoretical values correspond to microsolvation by 0−3 water molecules. [b] Theoretical values calculated at the B3LYP/6-31+G* level; values in parentheses are at the MP2 level and values in brackets are at B3LYP/6-31+G* PCM level. [c] Reference 6, 47. [d] Reference 52. [e] Reference 54. [f] Reference 55, 56.

TABLE 5: B3LYP/6-31+G* Calculated Activation Energies (kcal/mol)[a]

	n	Me	Et	i-Pr	t-Bu
gas	0	−0.9	2.8	5.3	11.7
propane	0	[9.4]	[14.3]	[17.2]	[24.3]
$\epsilon = 1.7$	1	1.1(0.1) [9.7]	4.6 (0.1) [13.7]	7.1 (0.2) [16.4]	13.2 (0.2) [23.4]
	2	2.7 (0.2) [7.4]	6.8 (0.3) [12.6]	8.6 (0.3) [15.0]	14.7 (0.3) [22.1]
ether	0	[16.3]	[20.8]	[23.7]	[30.0]
$\epsilon = 5.0$	1	1.9 (0.1) [15.8]	5.4 (0.1) [20.1]	7.9 (0.2) [22.6]	14.0 (0.2) [29.3]
	2	4.2 (0.3) [14.7]	7.6 (0.3) [21.6]	9.9 (0.3) [21.6]	16.0 (0.4) [28.1]
acetone	0	[19.8]	[24.4]	[27.4]	[33.9]
$\epsilon = 21.0$	1	2.7 (0.1) [18.1]	5.9 (0.2) [23.7]	8.4 (0.2) [25.0]	14.4 (0.2) [31.1]
	2	7.3 (0.3) [18.2]	10.8 (0.3) [22.1]	12.8 (0.3) [25.2]	18.6 (0.3) [30.6]
actonitrile	0	[20.0]	[24.5]	[27.6]	[34.1]
$\epsilon = 36.6$	1	4.0 (0.1) [20.0]	6.8 (0.1) [24.7]	9.6 (0.2) [27.1]	15.9 (0.2) [33.5]
	2	7.6 (0.2) [19.6]	10.7 (0.2) [24.0]	13.0 (0.3) [26.3]	18.8 (0.3) [31.8]
methanol	0	[20.8]	[25.0]	[27.2]	[33.2]
$\epsilon = 33.0$	1	5.0 (0.3) [21.9]	8.1 (0.3) [25.8]	10.5 (0.4) [27.5]	16.0 (0.5) [32.3]
	2	8.6 (0.6) [21.9]	11.8 (0.7) [25.7]	13.6 (0.8) [27.1]	18.2 (0.9) [31.2]
water	0	[21.2]	[25.4]	[27.7]	[33.8]
$\epsilon = 80.1$	1	4.5 (0.2) [20.6]	7.7 (0.3) [24.5]	10.1 (0.4) [26.5]	15.7 (0.2) [32.0]
	2	10.1 (0.6) [20.1]	13.2 (0.7) [24.0]	15.1 (0.8) [26.1]	20.0 (0.8) [30.3]

[a] Values in parenthesis are counterpoise estimates of the basis set superposition error. Values in brackets are B3LYP/6-31+G* PCM free energies.

displacement.[52] Furthermore, at least in DMF, the majority of substitution product is likely to arise via S_N1 or electron-transfer mechanisms,[22,24] making the experimental values in Table 4 lower bounds for the S_N2 barrier. In acetone the S_N1 mechanism is inhibited and the values of 6.0 and 7.6 kcal/mol are likely to be more reasonable estimates of the "true" S_N2 relative barrier. In any case, the data for the *tert*-butyl systems should be taken to be very approximative at best.

The experimental data indicate that the steric effect in solution is fairly independent of whether the nucleophile is Cl^- or Br^- or whether the solvent is DMF or acetone (neglecting the *tert*-butyl system, as discussed above). Table 4 shows that the steric effects in the gas phase are roughly twice those in acetone or DMF solutions.

The calculated changes in activation energy with 1−3 explicit water molecules show a clear trend of microsolvation reducing the steric effect. The results for $n = 4$ cannot be compared directly because there is no common solvation structure for the whole series. Inclusion of enthalpy corrections (mainly zero point energies, Supporting Information) causes a small decrease in the calculated effects, i.e. −0.1, −0.2, and −0.4 kcal/mol for ethyl, i-propyl, and *tert*-butyl, respectively, essentially independent of the number of water molecules. The results for the other solvents indicate similar but smaller effects than those for water, with the effect being approximately correlated with the macroscopic dielectric constant. This correlation indicates that it is reasonable to compare the computational results for microsolvation by water with the experimental data corresponding to macroscopic solvation by acetone or DMF.

It is notable that the PCM model alone ($n = 0$) is unable to account for changes in the steric effect upon solvation; it predicts values close to those in the gas phase. The PCM method has been parameterized to reproduce free energies and should therefore be compared to experimental relative free energies. Inclusion of entropy increases the steric effects by 0.7−0.8 and 1.4−1.9 kcal/mol for ethyl and i-propyl, respectively (no value is available for *tert*-butyl due to the dominance of the elimination reaction).[54−56] Although this improves the agreement, the PCM results are still less than quantitative. As discussed above, this is not due to the approximation of using fixed geometries, as the TS geometries change very little upon inclusion of water molecules for methyl, ethyl, and i-propyl. Table 2 shows that the electrostatic component increases slightly along the series, but it is almost canceled by the nonelectrostatic part. For the systems that include explicit water molecules, inclusion of the PCM correction reduces the steric effect, and even reverses the trend upon going from $n = 2$ to $n = 3$ for ethyl and i-propyl. We carried out a limited investigation of the sensitivity of the results to the parameters in the PCM method. Decreasing the atomic radii used for defining the cavity improves the results, but a reproduction of the experimental results requires radii significantly smaller than the van der Waals radii, which do not appear physically reasonable. This suggests that the PCM

TABLE 6: B3LYP/6-31+G* Calculated Relative Activation Energies (kcal/mol)[a]

	n	Me	Et	i-Pr	t-Bu
gas	0	0.0	3.6	6.2	12.6
propane	0	0.0	[3.9]	[7.7]	[14.9]
$\epsilon = 1.7$	1	0.0	3.5 [4.0]	6.0 [6.8]	12.1 [13.7]
	2	0.0	4.1 [5.2]	5.9 [7.6]	12.0 [14.7]
ether	0	0.0	[4.5]	[7.4]	[13.8]
$\epsilon = 5.0$	1	0.0	3.4 [4.3]	5.9 [6.8]	12.1 [13.5]
	2	0.0	3.5 [4.0]	5.8 [6.9]	11.8 [13.4]
acetone	0	0.0	[4.6]	[7.7]	[14.2]
$\epsilon = 21.0$	1	0.0	3.2 [4.6]	5.7 [7.0]	11.7 [13.1]
	2	0.0	3.3 [-]	5.5 [7.0]	11.2 [12.3]
actonitrile	0	0.0	[4.5]	[7.6]	[14.1]
$\epsilon = 36.6$	1	0.0	2.8 [4.7]	5.6 [7.1]	11.9 [13.5]
	2	0.0	3.1 [4.3]	5.5 [6.7]	11.3 [12.1]
methanol	0	0.0	[4.2]	[6.4]	[12.4]
$\epsilon = 33.0$	1	0.0	3.1 [3.8]	5.5 [5.6]	11.0 [10.4]
	2	0.0	3.2 [3.8]	5.0 [5.2]	9.6 [9.4]
water	0	0.0	[4.3]	[6.6]	[12.6]
$\epsilon = 80.1$	1	0.0	3.2 [3.9]	5.5 [6.0]	11.2 [11.4]
	2	0.0	3.1 [3.9]	5.0 [5.8]	9.9 [10.2]

[a] Values in brackets are B3LYP/6-31+G* PCM free energies.

TABLE 7: NPA Charges for the a Type TSs Calculated at B3LYP/6-31+G* Level Microsolvated by 0−3 Water Molecules

system	$n = 0$	$n = 1$	$n = 2$	$n = 3$
Me				
C	−0.50	−0.50	−0.49	−0.49
Cl	−0.64	−0.68	−0.61	−0.64
Cl	−0.64	−0.57	−0.61	−0.57
Et				
C	−0.23	−0.22	−0.22	−0.22
Cl	−0.68	−0.68	−0.66	−0.65
Cl	−0.64	−0.63	−0.66	−0.63
i-Pr				
C	0.04	0.05	0.06	0.07
Cl	−0.70	−0.72	−0.69	−0.70
Cl	−0.70	−0.66	−0.68	−0.67
t-Bu				
C	0.15	0.45	0.50	0.52
Cl	−0.65	−0.82	−0.82	−0.85
Cl	−0.64	−0.79	−0.81	−0.83

method should be used with care for estimating changes in activation energies due to steric effects.

Because the TSs for methyl, ethyl, and i-propyl display very few geometrical changes upon microsolvation, it is clear that the reduction in steric effect is not due to a loosening of the TS.[57] Table 7 shows calculated atomic charges for the **a** type TSs in water; very similar results are obtained for the other solvents. For the gas-phase reaction, the charge on the chlorine atoms increases for methyl, ethyl, and i-propyl but decreases again for *tert*-butyl. Microsolvation decreases the chlorine charges for methyl, ethyl, and i-propyl but causes a significant increase for the *tert*-butyl system. This is in accord with the geometrical changes, i.e., shortening $Cl-H_2O$ bonds upon methyl substitution and a significant lengthening of the C−Cl distances in the *tert*-butyl TS.

The implication is that the reduction in steric effect upon solvation for the methyl, ethyl, i-propyl, and *tert*-butyl series is due primarily to an increased solvation energy of the TS. The data in Table 7 suggest that the increased solvation is an indirect effect due to electron donation of the methyl groups, which increase the negative charges on the chlorines and thereby increase the strength of the interaction with the solvent. For the *tert*-butyl system, the TS displays a significant loosening upon microsolvation, which further increases the charge separation and leads to an additional solvent stabilization. Since the change in solvation energy along the series is due to explicit interaction with the solvent, it is not unexpected that the PCM method is problematic for modeling this effect.

VI. Conclusions

Solvation effects on the reaction profiles of S_N2 chlorine exchange reactions for methyl, ethyl, i-propyl, and *tert*-butyl have been studied using the B3LYP, MP2, and PCM methods. Microsolvation decreases the bonded C−Cl distances in the ion−dipole complex and increases the nonbonded C−Cl distances. The corresponding distances in the TSs increase with methyl substitution at the central carbon. For methyl, ethyl, and i-propyl, the TS geometries change very little upon microsolvation, but the *tert*-butyl system becomes significantly looser.

Inclusion of explicit water molecules decreases the stability of the ion−dipole complex, and the PCM results suggest that it disappears completely in bulk solution. The TS is less effective solvated than is the reactant due to charge delocalization, and the activation barrier consequently increases upon solvation. Relative activation energies are insensitive to the level of theory and clearly show that microsolvation decreases the steric effect. Both effects, the increase of absolute activation energies and reduction of relative activation energies compared to the gas phase, depend on the macroscopic dielectric constant of the solvent. The PCM method significantly underestimates this trend. Analysis of the data suggests that the reduction in steric effect upon solvation is due to the electron donating capability of the methyl groups at the central carbon. This leads to an increased charge on the chlorines in the TS and thereby to an increased interaction with the solvent.

Acknowledgment. This work was supported by grants from the Danish Natural Science Research Council. A.A.M. acknowledges a grant from the Danish *Rektorkollegiet*.

Supporting Information Available: Structures of solvated complexes for ethyl, i-propyl, and *tert*-butyl (3 figures). Tables of total energies thermodynamic corrections and atomic charges (7 Tables). This material is available free of charge via the Internet at http://pubs.acs.org.

References and Notes

(1) Hase, W. L. *Science* **1994**, *266*, 998.

(2) Chabinyc, M. L.; Carig, S. L.; Regan, C. K.; Brauman, J. I. *Science* **1998**, *279*, 1882.

(3) Shaik, S. S.; Schlegel, H. B.; Wolfe, S. *Theoretical Aspects of Physical Organic Chemistry and Mechanism*; Wiley: New York, 1992.

(4) Ingold, C. K. *Structure and Mechanism in Organic Chemistry*, 2nd ed.; Cornell University Press: Ithaca, 1969.

(5) Streitweiser, A., Jr. *Chem. Rev.* **1956**, *56*, 571. Detar, D. F.; Magnera, D. F.; Luthra, N. P. *J. Am. Chem. Soc*. **1978**, *100*, 2484. Riveros, J. M.; Jose, S. M.; Takashima, K. *Adv. Phys. Org Chem.* **1983**, *21*, 197.

(6) Caldwell, G.; Magenera, T. F.; Kebarle, P. *J. Am. Chem. Soc*. **1984**, *106*, 959.

(7) Tanaka, K.; Mackay, G. I.; Payzant, J. D.; Bohme, D. K. *Can. J. Chem*. **1976**, *54*, 1643.

(8) Bohme, D. K.; Rasket, A. B. *J. Am. Chem. Soc*. **1984**, *106*, 3447.

(9) Tomasi, J.; Persico, M. *Chem. Rev.* **1994**, *94*, 2027. Cramer, C. J.; Truhlar, D. J. In *Reviews in Computational Chemistry*; Lipowitz, K. B., Boyd B., Eds.; VCH: New York, 1995; Vol. 6, p 1.

(10) Cossi, M.; Barone, V.; Cammi, R.; Tomasi, J. *Chem. Phys. Lett*. **1996**, *211*, 327.

(11) Barone, V.; Cossi, M.; Tomasi, J. *J. Comput. Chem.* **1998**, *19*, 404.

(12) Cossi, M.; Barone, V. *J. Chem. Phys.* **1998**, *109*, 6246.

(13) Hayami, J.; Tanaka, N.; Hihara, N.; Kaji, A. *Tetrahedron Lett.* **1973**, 385.

(14) Hayami, J.; Koyanagi, T.; Hihara, N.; Kaji, A. *Bull. Chem. Soc. Jpn.* **1978**, 51, 891.

(15) Chandrasekhar, J.; Smith, S. F.; Jorgensen, W. L. *J. Am. Chem. Soc.* **1985**, *107*, 154. Chandrasekhar, J.; Smith, S. F.; Jorgensen, W. L. *J. Am. Chem. Soc.* **1984**, *106*, 3049.

(16) Chandrasekhar, J.; Jorgensen, W. L. *J. Am. Chem. Soc.* **1985**, *107*, 2974.

(17) Harris, J. M.; McManus, S. P., Eds.; *Nucleophilicity*; American Chemical Society: Washington, D.C., 1987.

(18) Hawang, J.-K.; King, G.; Creighton, S.; Warshel, A. *J. Am. Chem. Soc.* **1988**, *110*, 5297. Gertner, B. J.; Withnell, R. M.; Wilson, K. R.; Hynes, J. T, *J. Am. Chem. Soc.* **1991**, *113*, 74.

(19) Huston, S. E.; Rossky, P. J.; Zichi, D. A. *J. Am. Chem. Soc*. **1989**, *111*, 5680.

(20) Cossi, M.; Barone, V.; Adamo, C. *Chem. Phys. Lett*. **1998**, *297*, 1. Truong, T. N.; Stefanovich, V. *J. Phys. Chem.* **1995**, *99*, 14700. Re, M.; Laria, D. *J. Chem. Phys.* **1996**, *105*, 4584. Bennett, G. E.; Rossky P. J.; Johnston, K. P. *J. Phys. Chem.* **1995**, *99*, 16136. Luo, H.; Tucker, S. C. *J. Phys. Chem. B*, **1997**, *101*, 1063. Pomelli, C. S.; Tomasi, J. *J. Phys. Chem. A*, **1997**, *101*, 3561. Basilevsky, M. V.; Chdinov, G. E.; Napolov, D. V. *J. Phys. Chem*. **1993**, *97*, 3270.

(21) Okuno, Y. *J. Chem. Phys.* **1996**, *105*, 5817. Okuno, Y. *J. Am. Chem. Soc.* **2000**, *122*, 2925.

(22) Costentin, C.; Saveant, J.-M. *J. Am. Chem. Soc.* **2000**, *122*, 2329.

(23) Jensen, F. *Chem. Phys. Lett*. **1992**, *196*, 368.

(24) Okuno, Y. *J. Phys. Chem. A*, **1999**, *103*, 190. Mathis, J. R.; Kim, H. J.; Hynes, J. T. *J. Am. Chem. Soc.* **1993**, *115*, 8248.

(25) Gaussian 98, Frisch, M. J.; Trucks, G. W.; Schlegel, H. B.; Scuserie, G. E.; Robb, M. A.; Cheeseman, J. R.; Zakrzawski, V. G.; Montgomery, J. A.; Stratmann, R. E.; Burant, J. C.; Dapprich, S.; Millam, J. M.; Daniels, A. D.; Kudin, K. N.; Strain, M. C.; Farkas, O.; Tomasi, J.; Barone, V.; Cossi, M.; Cammi, R.; Mennucci, B.; Pomelli, C.; Adamo, C.; Califford, S.; Ochterski, J.; Petersson, G. A.; Ayala, P. Y.; Cui, Q.; Morokuma, K.; Malick, D. K.; Rabuck, A. D.; Raghavachari, K.; Foresman, J. B.; Cioslowski, J.; Ortiz, J. V.; Stefanov, B. B.; Liu, G.; Liashenko, A.; Piskorz, P.; Komaromi, I.; Gomperts, R.; Martin, R. L.; Fox, D. J.; Keith, T.; Al-Laham, M. A.; Peng, C. Y.; Nanayakkara, A.; Gonzalez, C.; Challacombe, M.; Gill, P. M. W.; Johnson, B. G.; Chen, W.; Wong, M. W.; Andres, J. L.; Head-Gordon, M.; Reploge, E. S.; Pople, J. A. Gaussian, Inc.: Pittsburgh, PA, 1998.

(26) Lee, C.; Yang, W.; Parr, R. G. *Phys. Rev. B* **1988**, *37*, 785. Becke, A. D. *Phys. Rev. A* **1988**, *38*, 3098. Becke, A. D. *J. Chem. Phys*. **1993**, *98*, 5648.

(27) Frisch, M. J.; Pople, J. A.; Binkley, J. S. *J. Chem. Phys*. **1984**, *80*, 3265.

(28) Deng, L.; Branchadell, V.; Ziegler, T. *J. Am. Chem. Soc*. **1994**, *116*, 10645.

(29) Abashkin, Y.; Russo, N. *J. Chem. Phys*. **1994**, *100*, 4477. Bell, R.; Truong, N. T. *J. Chem. Phys*. **1994**, *101*, 10442. Stanton, R. V.; Merz, K. M. Jr. *J. Chem. Phys*. **1994**, *101*, 7408. Zhang, Q.; Bell, R.; Truong, T. N. *J. Phys. Chem*. **1995**, *99*, 592.

(30) Alkorta, I.; Rosaz, I.; Egluero, J. *Chem. Soc. Rev*. **1998**, *27*, 163. Marek, L.; Danuta, R.; Hans-Georg, M. *J. Phys. Chem. A* **1997**, *101*, 1542. Puduzianowiski, A. T. *J. Phys. Chem*. **1996**, *100*, 4781. Van Bael, M. K.; Smets, J.; Schoane, K.; Houben, L.; McCarthy, W.; Maes, G.; Adamowicz, L.; Maciej, J. M. *J. Phys. Chem. A* **1997**, *101*, 2397.

(31) Kim, K.; Jordan, K. D. *J. Phys. Chem*. **1994**, *98*, 10089.

(32) Simon, S.; Duran, M.; Dannenberg, J. J. *J. Phys. Chem. A* **1999**, *103*, 1640.

(33) Bouteiller, Y.; Desfrancois, C.; Schermann, J. P.; Latajka, Z.; Silivi, B. *J. Chem. Phys.* **1998**, *108*, 7967.

(34) Kieninger, M.; Suhai, S. I. *Int. J. Quantum Chem.* **1994**, *52*, 465.

(35) Odutola, J. A.; Dyke, T. R. *J. Chem. Phys.* **1980**, *72*, 5062.

(36) Miertus, S.; Scrocco, E.; Tomasi, J. *Chem. Phys.* **1981**, *55*, 117. Cossi, M.; Mennucci, B.; Tomasi, J. *Chem. Phys. Lett*. **1994**, *228*, 165.

(37) Reed, A. E.; Curtiss, L. A.; Weinholt, F. *Chem. Rev.* **1988**, *88*, 899.

(38) Xantheas, S. S.; Dunning, T. H., Jr. *J. Phys. Chem.* **1994**, *98*, 13489.

(39) Keesee, R. G.; Castlman, A. W., Jr. *J. Phys. Chem. Ref. Data* **1986**, *15*, 1018.

(40) Tucker, S. C.; Truhlar, D. G. *J. Am. Chem. Soc.* **1990**, *112*, 3338. Tucker, S. C.; Truhlar, D. G. *J. Am. Chem. Soc.* **1990**, *112*, 3347.

(41) Pearson, R. G. *J. Am. Chem. Soc.* **1986**, *73*, 115.

(42) Truong, T. N.; Stefanovich, E. V. *J. Phys. Chem.* **1995**, *99*, 14700.

(43) Larson, J. W.; McMahon, J. B. *J. Am. Chem. Soc.* **1984**, *106*, 517.

(44) Doughwerty, R. C.; Dalton, J.; Roberts, *J. Org. Mass. Spectrom.* **1974**, *83*, 77.

(45) Han, C.-C.; Dodd, J. A.; Brauman, J. I. *J. Phys. Chem.* **1986**, *90*, 471. Gonert, S.; Depuy, C. H.; Bierbaum, V. M. *J. Am. Chem. Soc.* **1991,** *113*, 4009.

(46) Barlow, S. E.; Doren, J. M. V.; Bierbaum, V. M. *J. Am. Chem. Soc.* **1988**, *110*, 7240.

(47) Botschwina, P. *Theor. Chem. Acc.* **1998**, *99*, 426.

(48) Hirao, K.; Kebarle, P. *Can. J. Chem.* **1989**, *67*, 1261.

(49) Morokuma, K. *J. Am. Chem. Soc.* **1982**, *104*, 3732.

(50) Albery, W. J.; Kreevoy, M. M. *Adv. Phys. Org. Chem.* **1978**, *16*, 87.

(51) Kong, Y. S.; Jhon, M. S. *Theor. Chim. Acta* **1986**, *70*, 123.

(52) Albery, W. J. *Annu. Rev. Phys. Chem.* **1980**, *31*, 227.

(53) van Duijneveldt, F. B.; van Duijneveldt-van der Rijdt, J. G. C. M.; van Lenthe, J. H. *Chem. Rev.* **1994**, *94*, 1873.

(54) Cook, D.; Parker, A. J. *J. Chem. Soc. B* **1968**, 142.

(55) Hughes, E. D.; Ingold, C. K.; Mackie, J. D. H. *J. Chem. Soc*. **1955**, 3173.

(56) De la Mare, P. B. D. *J. Chem. Soc.* **1955**, 3180.

(57) Parker, A. J. *Chem. Rev.* **1969**, *69*, 1.